ACTA ABP BIOCHIMICA POLONICA

Vol. 57, No 3/2010
355–360
on-line at: www.actabp.pl

Regular paper

Depletion of intracellular glutathione and increased lipid peroxidation mediate cytotoxicity of hematite nanoparticles in MRC-5 cells*

Mihaela Radu[1], Maria Cristina Munteanu[1], Sorina Petrache[1], Andreea Iren Serban[2], Diana Dinu[1], Anca Hermenean[3], Cornelia Sima[4] and Anca Dinischiotu[1]✉

[1]Department of Biochemistry and Molecular Biology, Faculty of Biology, University of Bucharest, Bucharest, Romania; [2]Departament of Preclinical Sciences, Faculty of Veterinary Medicine, University of Agricultural Sciences and Veterinary Medicine, Bucharest, Romania; [3]Department of Histology, Vasile Goldis Western University of Arad, Arad, Romania; [4]Laser Department, National Institute of Laser, Plasma and Radiation Physics, Bucharest-Magurele, Romania

Particles generated from numerous anthropogenic and/or natural sources, such as crystalline α-Fe_2O_3 nanoparticles, have the potential to damage lung cells. In our study we investigated the effects of these nanoparticles (12.5 μg/ml) on lipid peroxidation and the antioxidative system in MRC-5 lung fibroblast cells following exposure for 24, 48 or 72 h. Exposure to α-Fe_2O_3 nanoparticles increased lipid peroxidation by 81%, 189% and 110% after 24, 48 and 72 h, respectively. Conversely, the reduced glutathione concentration decreased by 23.2% and 51.4% after 48 and 72 h of treatment, respectively. In addition, an augmentation of the activities of superoxide dismutase, catalase, glutathione peroxidase, glutathione transferase and glutathione reductase within the interval between 48–72 h was noticed. Taking into account that the reduced glutathione level decreased and the malondialdehyde level, a lipid peroxidation product, remained highly increased up to 72 h of exposure, it would appear that the MRC-5 antioxidant defense mechanisms did not efficiently counteract the oxidative stress induced by exposure to hematite nanoparticles.

Keywords: hematite nanoparticles, MRC-5 cells, lipid peroxidation, glutathione, antioxidant enzymes

Received: 08 March, 2010; revised: 26 June, 2010; accepted: 16 August, 2010; available on-line: 11 September, 2010

INTRODUCTION

Human lungs are in permanent contact with the environment, being one of the entry points for natural or anthropogenic nanoparticles, which have at least one dimension smaller than one micrometer. Due to their small dimensions, the nanometer-sized particles can penetrate the lung barrier and enter the human circulatory and lymphatic systems, becoming dispersed in different organs, tissues and cells. The effects of nanoparticles on cellular processes mainly depend on their size, chemical composition, crystallinity, aggregation, including a potential contribution to the development of lung and neurodegenerative diseases (Buzea *et al.*, 2007).

Iron oxides exist in many forms in nature, with magnetite (Fe_3O_4), maghemite (γ-Fe_2O_3), and hematite (α-Fe_2O_3) being probably the most common (Cornell & Schwertmann, 2003). Furthermore, iron and other metal oxides nanoparticles are constituents of volcanic ash (Yano *et al.*, 1990). In an aqueous medium containing iron complexes magnetite nanoparticles can be synthesized under aerobic conditions in the presence of *Actinobacter* spp. (Bharde *et al.*, 2005).

Prepared nanoparticles are often used as industrial catalysts (Oberdorster *et al.*, 2005). Their elevated levels at sites surrounding industrial plants and in the gravitation dust sediments of residential agglomeration (Flórián *et al.*, 2003) combined with the dynamics of dust migration across large distances (Buzea *et al.*, 2007) enhance human exposure.

Nanoparticles such as Fe_3O_4 (Hernández *et al.*, 2009) or Fe_2O_3 (Sevilla *et al.*, 2009) were used previously for the preparation of efficient magnetic nanocomposites for de-contamination of persistent organic pollutants and arsenic (Giasuddin *et al.*, 2007). All three forms of iron oxide are also used in synthetic pigments in paints, ceramics, and porcelain (Cornell & Schwertmann, 2003).

Unintentional inhalation due to air pollution or application of products containing iron nanoparticles, as well as unavoidable exposure in the workplace, can generate cellular responses in lungs and other organs that may cause significant public health problems (Donaldson *et al.*, 2005; Powell & Kanarek, 2006).

The pathways involved in the internalization of nanoparticles into cells are: clathrin-mediated transport (Stearns *et al.*, 2001), caveolae-dependent endocytosis (Műhlfeld *et al.*, 2008), macropinocytotic uptake (Shukla *et al.*, 2005), as well as other mechanisms in which adhesive interactions due to electrostatic forces, Van der Waals or steric interactions (Green *et al.*, 2000, Rothen-Rutishauser *et al.*, 2007) are involved. Once they enter human cells, iron oxide nanoparticles induce reactive oxygen species (ROS) production (Apopa *et al.*, 2009) and oxidative stress.

According to Klotz and Sies (2009), nanoparticles can generate ROS by different mechanisms. Consequently, the uptaken metal oxide nanoparticles can lose the me-

✉e-mail: dinischiotu@yahoo.com; adin@bio.unibuc.ro

*The present work was accepted as poster presentation at IUTOX 2010 Barcelona, 19–23 July.

Abbreviations: CAT, catalase; CDNB, 1-chloro-2, 4-dinitrobenzene; GR, glutathione reductase; GPX, glutathione peroxidase; GSH, reduced glutathione; GST, glutathione-S-transferase; MDA, malondialdehyde; MEM, modified Eagle's medium; MTT, 3-(4, 5-dimethylthiazol-2-yl)-2,5-diphenyltetrazolium bromide; ROS, reactive oxygen species; SOD, superoxide dismutase

tallic ions. Iron, being a highly redox-active transition metal, can be involved in the Fenton reaction producing hydroxyl radicals. These nano-sized particles could directly interact with NADPH oxidases from the plasma membrane and/or mitochondria thus disturbing the electron transport chain and generating a superoxide anion. It is also possible that the nanoparticle-induced damage of the mitochondria and endoplasmic reticulum could determine Ca^{2+} release into the cytosol, where several Ca^{2+}/calmodulin dependent enzymes, such as nitrogen monoxide synthase isoforms, become activated, resulting in production of nitric oxide and peroxynitrite.

Both *in vitro* and *in vivo* studies of the health effects of ambient nano-materials have identified the generation of oxidative stress as one of the major mechanisms by which air pollution particles exert adverse biological effects.

Cellular redox homeostasis is carefully maintained by an elaborate antioxidant defense system which includes antioxidant enzymes, proteins, and low-molecular-mass scavengers. Excessive ROS production or weakening of antioxidant defense could lead to oxidative stress. Oxidative stress is a redox disequilibrium in which ROS and lipid radicals attack proteins and nucleic acids, redox-sensitive signaling cascades being activated (Li *et al.*, 2003). The late cellular response is represented by pro-inflammatory effects (Jeng & Swanson, 2006) and cytotoxicity (Nel *et al.*, 2006).

The aim of this study was to evaluate the oxidative stress mechanisms induced by α-Fe_2O_3 nanoparticles in human lung fibroblast cell line MRC-5. The malondialdehyde (MDA) and reduced glutathione (GSH) levels as well as the activities of antioxidant enzymes, such as superoxide dismutase (SOD), catalase (CAT), glutathione peroxidase (GPX), glutathione reductase (GR) and glutathione-*S*-transferase (GST) were also analyzed.

MATERIALS AND METHODS

Chemicals. GIBCO® Modified Eagle's Medium (MEM), fetal bovine serum, gentamycin (10 mg/ml), L-glutamine and vitamin solution (100×) were purchased from Invitrogen (Carlsbad, California, USA). Nicotinamide adenine dinucleotide phosphate disodium salt ($NADP^+$) and nicotinamide adenine dinucleotide phosphate reduced tetrasodium salt (NADPH) were from Merck (Darmstadt, Germany). Tetraethoxypropane (TEP) and thiobarbituric acid (TBA) were obtained from Fluka (Milwaukee, USA). The Detect X® Glutathione Colorimetric Detection Kit was purchased from Arbor Assay (Michigan, USA). Other chemicals used were of analytical grade and were from Sigma (St. Louis, Missouri, USA).

Nanoparticles. Nanoparticles of the α form of Fe_2O_3 (hematite) were obtained by laser reactive ablation in the Laser Department of the National Institute of Laser, Plasma and Radiation Physics (Bucharest-Măgurele, Romania). The particle size assessment was performed with a high resolution transmission electron microscope (Philips CM120 model). The primary nanoparticle size distribution was lognormal in the range 10–120 nm, most of them measuring 40–60 nm. For crystallinity analysis Bruker AXS/D8 ADVANCE X ray diffractometer was used.

Cell lines and treatment. MRC-5 cells were maintained in MEM containing non-essential amino acids, Earle's salts, L-glutamine and 10% fetal bovine serum. Cells, between passages 11–20, were grown as monolayers in a humidified 5% CO_2 air atmosphere at 37 °C in 75 cm^2 culture flasks. They were seeded at a density of 2.5×10^5 cells/ml. Stock suspensions of α-Fe_2O_3 nanoparticles were sterilized before use. In each experiment, the stock suspensions were sonicated and freshly diluted to appropriate concentrations in the cell medium. The cells were incubated with hematite nanoparticles at concentrations of 2.5 μg/ml, 6.25 μg/ml, or 12.5 μg/ml in the culture medium for 24, 48, and 72 h. Controls without treatment were performed for each experiment.

Cell viability assay. The viability of the cells was determined by the tetrazolium salt test (Mosmann, 1983). The medium from each well was removed by aspiration, the cells were washed with 200 μl of phosphate-buffered saline (PBS)/well and then 50 μl (1 mg/ml) of 3-(4, 5-dimethylthiazol-2-yl)-2,5-diphenyltetrazolium bromide (MTT) solution was added to each well. After 2 h of incubation the MTT solution from each well was removed by aspiration. A volume of 50 μl isopropanol was added and the plate was shaken to dissolve the formazan crystals. The absorbance at 595 nm, was then determined using a Tecan multiplate reader (Tecan GENios, Grödic, Germany), for each well. The absorbance for untreated cells was taken to represent the 100% viability.

Preparation of cell lysate. MRC-5 cells were harvested from culture flasks, after the removal of medium which contained the floating dead cells, washed with PBS and centrifuged at $1\,500 \times g$ for 10 min at 4 °C. Cell pellets were re-suspended in 0.5 ml of PBS and then sonicated on ice three times, for 30 s each. The total extract was centrifuged at $3\,000 \times g$ for 15 min at 4 °C. Aliquots of the supernatant were used for enzyme assays.

Lipid peroxidation. MDA, as an *in vitro* marker of lipid peroxidation, was assessed by a method described by Del Rio *et al.* (2003). To 200 μl of sample with a protein concentration of 2 mg/ml, 700 μl of 0.1 M HCl was added and the mixture was incubated for 20 min at room temperature. Then, 900 μl of 0.025 M thiobarbituric acid (TBA) was added and the mixture was incubated for 65 min at 37 °C. Finally, 400 μL of 10 mM PBS was added. The fluorescence of MDA was recorded using a 520/549 (excitation/emission) filter. A calibration curve with MDA in the range 0.05–5 μM was used to calculate the MDA concentration. The results were expressed as nmoles of MDA/mg protein.

Glutathione assay. The cellular lysate, deproteinized with 5% sulfosalicylic acid, was analyzed for total glutathione and oxidized glutathione (GSSG) using the Detect X® Glutathione colorimetric detection kit and following manufacturer's instructions. GSH concentration is obtained by subtracting the GSSG level from the total glutathione. The total and GSH levels were calculated as nmoles/mg protein.

Antioxidant enzymes assay. Total SOD (EC 1.15.1.1) activity was measured according to the spectrophotometric method of Paoletti *et al.* (1986), based on NADPH oxidation by the superoxide anion generated from molecular oxygen by a purely chemical reaction in the presence of EDTA, manganese (II) chloride and mercaptoethanol. The decrease in absorbance at 340 nm due to NADPH oxidation was followed for 10 min. A control was run with each set of three duplicate samples and the percent inhibition was calculated as (sample

rate)/(control rate) ×100. One unit (U) of activity was defined as the amount of enzyme required to inhibit the rate of NADPH oxidation of the control by 50%.

The CAT (EC 1.11.1.6) activity was assayed by monitoring the disappearance of H_2O_2 at 240 nm, according to the method of Aebi (1984). The CAT activity was calculated in terms of U/mg protein, where one unit (U) is the amount of enzyme catalyzing the conversion of one µmole of H_2O_2 in a minute under standard condition of temperature, optimal pH and optimal substrate concentration.

Total GPX (EC 1.11.1.9) was assayed by the Beutler method (1971), using tert-butyl hydroperoxide and NADPH as substrates. The conversion of NADPH to $NADP^+$ was followed by recording the changes in absorbance at 340 nm, and the concentration of NADPH was calculated using a molar extinction coefficient of 6.22×10^3 $M^{-1} \cdot cm^{-1}$. The activity was expressed as U/mg. One unit of activity was defined as the amount of enzyme that catalyzes the conversion of one µmole of NADPH per minute under standard conditions.

The GR (EC 1.6.4.2) activity was measured according to the method of Goldberg and Spooner (1983), in 0.1 M phosphate buffer, pH 7.4 with 0.66 mM GSSG and 0.1 mM NADPH by recording the decrease of absorbance at 340 nm. The activity of this enzyme was expressed as U/mg, one unit of GR activity been defined as one µmole of NADPH per minute under standard conditions.

The GST (EC 2.5.1.18) activity was assayed spectrophotometrically at 340 nm by measuring the rate of CDNB conjugation with GSH, according to the method of Habig *et al.* (1974), and calculated as U/mg. One unit of GST activity was defined as the amount of enzyme that catalyzed the transformation of one µmole of CDNB in conjugated product per minute. The extinction coefficient 9.6×10^3 $M^{-1} \cdot cm^{-1}$ was used for the calculation of CDNB concentration.

All enzymatic activities, calculated as specific activities (units/mg protein) are expressed as percentage of controls.

Protein concentration. The protein concentration (mg/ml) was determined by the method of Bradford (1976), using bovine serum albumine as a standard.

Statistical analysis. The differences between control and α-Fe_2O_3 nanoparticles-treated cells were compared by Student's *t*-test using standard statistical packages. All data were expressed as means (n=4) ± standard deviation (S.D.) and differences were considered significant from control at $P<0.05$, highly significant at $P<0.01$ and extremely significant at $P<0.001$.

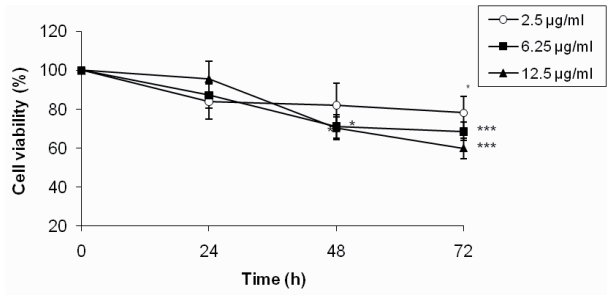

Figure 1. Viability of MRC-5 cells following exposure to α-Fe_2O_3 nanoparticles
The values shown are means ±S.D. (n=6) and expressed as percentage of time-interval controls *$P<0.05$; ***$P<0.001$.

RESULTS

Cell viability

The hematite nanoparticles decreased the number of viable MRC-5 cells in a time- and dose-dependent manner (Fig. 1). The incubation of cells with 2.5 µg/ml of α-Fe_2O_3 did not cause a significant loss of viability after 24h or 48h, and a decrease by 22% after 72h. The decrease in cell viability induced by the exposure to 6.25 µg/ml α-Fe_2O_3 was between 29% after 48h and 31.5% after 72h. After the treatment of MRC-5 cells with the highest α-Fe_2O_3 concentration of 12.5 µg/ml, the viability decreased by 10% after 24h, and by 30% and 44% after 48h and 72h, respectively.

Taking into account that the most pronounced effects were noticed at the highest concentration tested (12.5 µg/ml), this was used in all subsequent experiments.

Lipid peroxidation

The exposure of MRC-5 cells to hematite nanoparticles increased the MDA concentration in a time-dependent manner by 81%, 189% and 110% after 24, 48 and 72h, respectively (Table 1). As it can be seen in Table 1, the MDA level continuously increased in the first 48h of exposure and started decreasing after 72h, but still remained high in comparison with control.

Total and reduced glutathione depletion

The results shown in Table 1 indicate that exposure of MRC-5 cells to Fe_2O_3 nano-sized particles resulted in a slight diminution in the total glutathione level by 17.7% after 48h, followed by a decline by 51.4% after 72h. The same tendency was noticed for the GSH con-

Table 1. Lipid peroxidation, total glutathione and GSH concentrations in MRC-5 cells after treatment with 12.5 µg/mL α-Fe_2O_3
Values are means ±S.D. (n=4)

Time (hours)	Sample	Total glutathione (nmoles/mg)	GSH (nmoles/mg)	Lipid peroxidation (nmoles MDA/mg)
24	Control	25.62±0.36	23.23±0.11	0.021±0.004
	α-Fe2O3 nanoparticles	26.57±0.34	22.65±0.17	0.038±0.002*
48	Control	30.67±0.17	27.82±0.18	0.019±0.004
	α-Fe_2O_3 nanoparticles	25.24± 0.28**	21.35±0.26**	0.055±0.002***
72	Control	31.52±0.12	25.32±0.33	0.020±0.002
	α-Fe_2O_3 nanoparticles	15.23±0.17***	12.24±0.29***	0.042±0.003***

*$P<0.05$; **$P<0.01$; ***$P<0.001$.

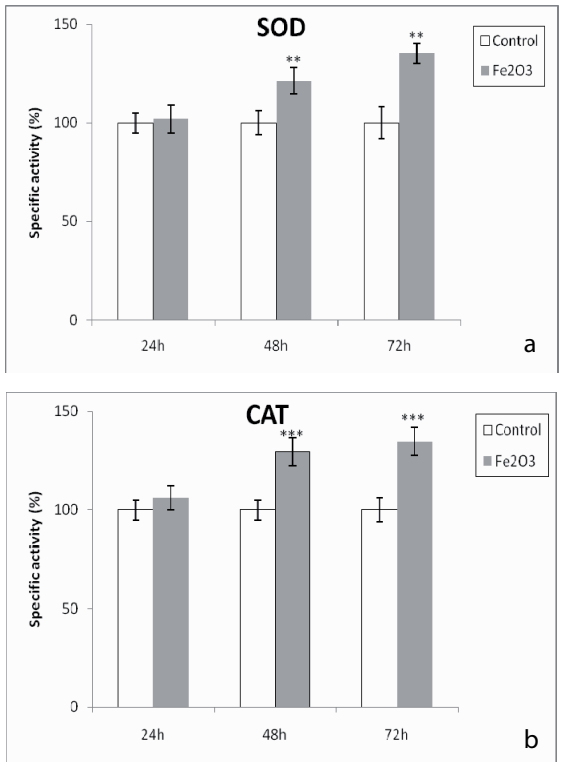

Figure 2. Effects of exposure to α-Fe_2O_3 nanoparticles on the activities of SOD (a) and CAT (b) in MRC-5 cells
The values are calculated as means ± S.D. (n = 4) and expressed as percentage of controls. $^{**}P < 0.01$; $^{***}P < 0.001$.

tent which decreased by 23.2% and 51.4% after 48 h and 72 h of treatment, respectively.

The antioxidant scavenging enzymes

Figures 2a and 2b show the effects of α-Fe_2O_3 nanoparticles on the activities of antioxidant enzymes, SOD and CAT in MRC-5 cells. The SOD activity increased by 21.2% and 35.1% after 48 h and 72 h, and for the same time points, the activity of CAT was up-regulated by 29.5% and 34.7%, respectively; however, no significant changes were noticed after 24 h.

After 24 h of exposure to hematite nanoparticles, no significant changes of the specific activities of GPX, GR and GST were visible.

Beginning at 48 h of exposure, an increase in GPX, GR and GST activities was noticed (Figs. 3a, 3b, 3c): by 52% and 37% for GPX activity, by 21% and 32% for GST, and by 13% and 21% for GST after 48 h and 72 h of treatment, respectively.

DISCUSSION

This study was initiated in order to evaluate the antioxidative capacity of MRC-5 lung fibroblasts exposed to hematite nanoparticles, taking into account that human occupational and environmental exposures to these is common. In our study, nanoparticles between 40 nm and 60 nm were dominated in the preparation used. Such particles have high coefficient of diffusion leading to efficient deposition probability at airways bifurcation and centers of lung acini (Churg & Vedal, 1996), before they

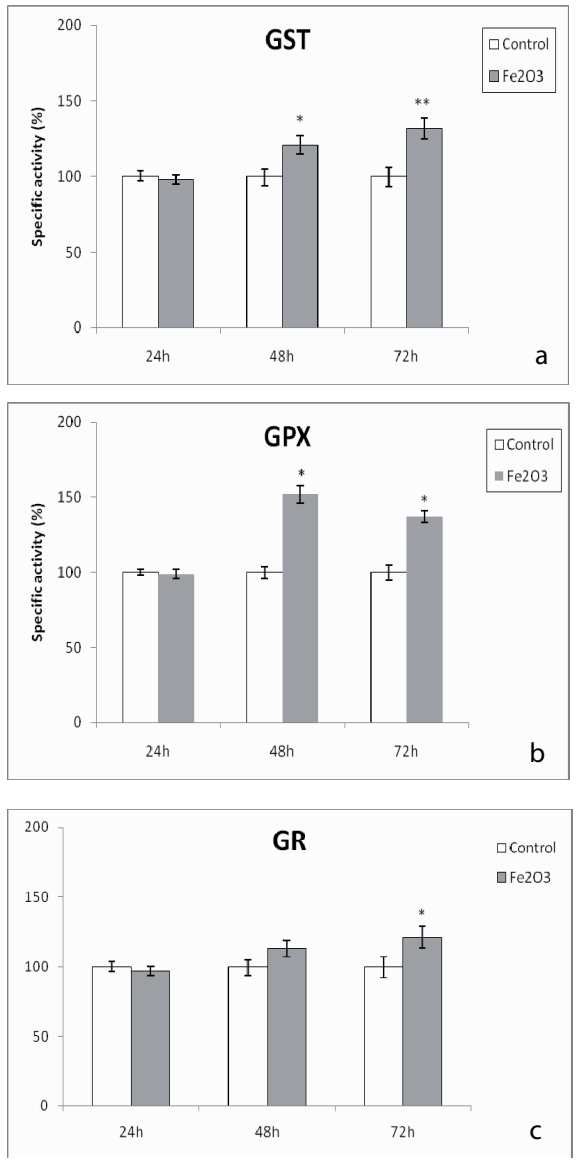

Figure 3. Effects of exposure to α-Fe_2O_3 nanoparticles on GST (a) and GPX (b) and GR (c) activities in MRC-5 cells
The values are means ± S.D. (n = 4) and expressed as percentage of controls. $^{*}P < 0.05$; $^{**}P < 0.01$.

are transported to the deep lung (Maynard & Kuempel, 2005).

Hematite is insoluble at a physiological temperature and pH (Diakonov *et al.*, 1999), but interfacial hydration of anhydrous hematite results in higher solubility (Jang *et al.*, 2007). On the other hand, αFe_2O_3 nanoparticles could release some ferric ions once they enter the cells, as previously noticed for other types of ultrafine particles (Wang *et al.*, 2008). Subsequently, these ions would be able to interact with hydrogen peroxide physiologically formed by different types of enzyme-catalyzed reactions, generating hydroperoxyl radical (Hurd & Murphy, 2009) according to the reaction:

$$Fe^{3+} + H_2O_2 \rightarrow Fe^{2+} + H^+ + HOO^{\cdot} \quad (1)$$

Ferrous ions also participate in the Fenton reaction, generating a hydroxyl radical.

Three possible mechanisms have been put forward to explain superoxide anion generation in MRC-5 cells, af-

ter nano-sized hematite enters the cells. First, the uptaken nanoparticles could interact with NADPH oxidase in the plasma membrane, thus generating superoxide in the extracellular space (Dhaunsi *et al.*, 2004), which would enter the cell through an anion channel (Bedard & Krause, 2007). Second, these nanoparticles could interact with a recently identified NADPH oxidase isoform located in the endoplasmatic reticulum (Chen *et al.*, 2008), forming this oxygen radical endogenously. And third, small quantities of Fe^{3+} ions released from these nanoparticles in the cytosol, could be reduced to Fe^{2+} according to reaction (1) and imported into the mitochondrial matrix through orthologs of Mrs3/Mrs4 transporters (Froschauer *et al.*, 2009) in vertebrates. The mitochondrial iron accumulation appears to be ensued by oxidative damage (Crichton *et al.*, 2002). The labile iron pool present within mitochondria (Kruszewski, 2004) together with the decrease of reduced glutathione level could impair the biogenesis of iron-sulfur clusters within the matrix (Hausmann *et al.*, 2005). These iron-sulfur clusters are present in different mitochondrial proteins including some of the mitochondrial electron transport chain. At the ultrastructural level, Complexes I and III are the main sites of mitochondrial superoxide production. It has been demonstrated that Complex I-dependent superoxide is exclusively released into the matrix whereas Complex III releases superoxide to both sides of the inner mitochondrial membrane (Muller *et al.*, 2004). In Complex I, the most likely sites of electron leakage are the iron sulfur clusters (Barja, 1999).

Several enzymatic defense mechanisms attempt to minimize the production and the action of harmful oxidants, such as SOD, CAT and GPX.

SOD dismutates the free radical superoxide by converting it to hydrogen peroxide, which in turn is decomposed by CAT at high concentration, and by GPX at low concentration. In our experiment, the activities of SOD and CAT increased after 48h and remained at almost same levels for the next 24h. Most hydrogen peroxide in the cell is generated through the dismutation of superoxide by SOD action, even though it can be produced by other superoxide-generating enzymes (Hauptmann *et al.*, 1996; Arimoto *et al.*, 2005). It was proved that lung edema was markedly supressed by pretreatment with polyethylene glycol-modified superoxide dismutase (Sagai *et al.*, 1993). Probably, the generation of superoxide becomes critical in a time-dependent manner, and so the induction of SOD activity is important only after 48h of exposure to hematite nanoparticles. Despite the good correlation between the SOD and CAT activities in MRC-5 cells, some superoxide and hydrogen peroxide could remain in the cells.

The superoxide anions that escape dismutation can react with hydrogen peroxide according to Haber–Weiss reaction to form hydroxyl radicals or become protonated to hydroperoxyl radicals. Hydroperoxyl and hydroxyl radicals are able to abstract hydrogen atom from a methylene group adjacent to double bonds of polyunsaturated fatty acids forming carbon centered radicals that react with molecular oxygen to form lipid peroxides (Antunes *et al.*, 1996). The significant increase of MDA concentration, by 189% and 110% after 48h and 72h, respectively, suggests that the antioxidative system adaptation was not sufficient to prevent damage of membrane lipids; in turn, the lipid peroxidation products could affect the structure of DNA bases (Valko *et al.*, 2006), proteins and carbohydrates. Similar results were obtained in human bronchial epithelial BEAS-2B cells exposed to TiO_2 nanoparticles (Gurr *et al.*, 2005) and ZnO ones (Yang *et al.*, 2009) whereas in A549 human lung epithelial cells treated with maghemite nano-sized particles, the change in lipid peroxidation variation was statistically insignificant (Guo *et al.*, 2009).

The enzymes of the glutathione redox cycle, comprising GPX, GR and GST, are another source of protection against oxidative stress. GPX and GST, the enzymes that reduce the levels of peroxides thereby protecting the cell from peroxidative damages, showed similar responses during exposure to α-Fe_2O_3 nanoparticles. An activation of GPX was observed, with the maximum at 48h of about 152% compared to the time-interval control; subsequently, the activity of this enzyme decreased to 137% of the control at 72h. The decrease in GPX activity could suggest inactivation by ROS, whose level increased in MRC-5 cells after 72h. Superoxide anions have been shown to inhibit GPX (Blum & Fridovich, 1985). Accordingly, the antioxidant defense system of MRC-5 cells reacted positively to α-Fe_2O_3 nanoparticles toxicity by increasing the GST activity. The family of GSTs contains enzymes that are capable of multiple reactions with a multitude of substrates in order to detoxify the endogenous compounds, such as peroxidised lipids, as well as the metabolism of xenobiotics.

The increase of the GPX and GST activities may be correlated with the observed decrease in GSH content of MRC-5 cells. Thus the decrease in the level of GSH after 48h of α-Fe_2O_3 nanoparticle treatment may be explained by its use as a substrate of GPX. The increased participation of GSH in conjugation reactions mediated by increased GST activity seems to be a plausible explanation for the reduced GSH content (51.4% from time interval control) after exposure to α-Fe_2O_3 nanoparticles for 72h. Other noticeable changes concerning the enzymatic antioxidant response to the nanoparticles-linked oxidative stress were registered in the specific activity of GR, an enzyme involved in the recycling of GSSG to GSH. Nevertheless, this enzymatic adaptation was insufficient to prevent the significant reduction of the GSH concentration in MRC-5 cells after 72h of treatment, which suggested an oxidative stress condition. On the other hand, ferric ions at high concentrations, being electrophilic, can deplete intracellular reduced glutathione by interacting with sulfhydryl groups (Brodie *et al.*, 1982) or by inhibition of several cellular activities including the cystine uptake (Bannai, 1984). Also, the long exposure to hematite nanoparticles could induce the loss of cellular GSH by glutathionylation of several proteins (Hare & Stamler, 2005).

In conclusion, taking into account that the GSH concentration decreased and MDA level remained highly increased up to 72h of treatment, it appears that the MRC-5 antioxidant defense mechanisms do not efficiently counteract the oxidative stress induced by exposure to hematite nanoparticles and possible damaging effects could occur.

Acknowledgement

This study was financially supported by the National Research Council of Higher Education, Romania, Grant number 340/2007 and Grant POSDRU 8/1.5/S/61150/2010 co-financed from European Social Fund by the Sectorial Operational Program for Development of Human Resources 2007-2013. The authors are grateful to COST B35/2006 Action for the opportunity to exchange ideas with experts in lipid peroxidation and oxidative stress.

REFERENCES

Aebi H (1984) Catalase *in vitro*. In *Methods of enzymatic analysis*. Bergmayer HU, ed, pp 673–684. Weinheim, FRG.

Antunes F, Salvador A, Marinho HS, Alves R, Pinto RE (1996) Lipid peroxidation in mitochondrial inner membranes. I. An integrative kinetic model. *Free Rad Biol Med* **21:** 917–943.

Apopa PL, Qian Y, Shao R, Lan Guo N, Schwegler-Berry D, Pacurari M, Porter D, Shi X, Vallayathan V, Castranova V, Plynn DC (2009) Iron oxide nanoparticles induce human microvascular endothelial cell permeability through reactive oxygen species production and microtubule remodeling. *Part Fibre Toxicol* **6:** 1.

Arimoto T, Kadiiska MB, Sato K, Corbett J, Mason RP (2005) Synergistic production of lung free radicals by diesel exhaust particles and endotoxin. *Am J Respir Crit Care Med* **171:** 379–387.

Bannai S (1984) Transport of cystine and cysteine in mammalian cells. *Biochim Biophys Acta* **779:** 289–306.

Barja G (1999) Mitochondrial oxygen radical generation and leak**:** sites of production in states 4 and 3, organ specificity and relation to aging and longevity. *J Bioenerg Biomembr* **31:** 347–366.

Bedard K, Krause KH (2007) The NOX family of ROS-generating NADPH oxidases: physiology and pathophysiology. *Physiol Rev* **87:** 245–313.

Beutler E (1971) Red cell metabolism. In *A manual of biochemical methods*, eds, pp 71–73. Grune & Stratton, New York.

Bharde A, Wani A, Shouche J, Joy PA, Prasad BL, Sastry S (2005) Bacterial aerobic synthesis of nanocrystalline magnetite. *J Am Chem Soc* **127:** 9326–9327.

Blum J, Fridovich I (1985) Inactivation of glutathione peroxidase by superoxide radical. *Arch Biochem Biophys* **240:** 500–508.

Bradford MM (1976) A rapid and sensitive method for the quantitation of microgram quantities of protein utilizing the principle of protein-dye binding. *Anal Biochem* **72:** 248–254.

Brodie AE, Potter J, Reed DJ 1(982) Unique characteristics of rat spleen lymphocyte, L1210 lymphoma and HeLa cells in glutathione biosynthesis from sulfur-containing amino acids. *Eur J Biochem* **123:** 159–164.

Buzea C, Pacheco II, Robbie K (2007) Nanomaterials and nanoparticles: sources and toxicity. *Biointerphases* **2:** MR17–MR71.

Chen K, Kirber MT, Xiao H, Yang Y, Keaney JF Jr (2008) Regulation of ROS signal transduction by NADPH oxidase 4 localization. *J Cell Biol* **181:** 1129–1139.

Churg A, Vedal S (1996) Carinal and tubular airway particle concentrations in the large airways of non-smokers in the general population: Evidence for high particle concentration at airways carinas. *Occup Environ Med* **53:** 553–558.

Cornell RM, Schwertmann U (2003) *The iron oxides: Structure, properties, reactions, occurrences and uses*, pp 2–3. Wiley-VCH Verlag, Weinheim, Germany.

Crichton RR, Wilmet S, Legssyer R, Ward RJ (2002) Molecular and cellular mechanisms of iron homeostasis and toxicity in mammalian cells. *J Inorg Biochem* **91:** 9–18.

Del Rio D, Pellegrini N, Colombi B, Bianchi M, Serafini M, Torta F, Tegoni M, Musci M, Brighenti F (2003) Rapid fluorimetric method to detect total plasma malondialdehyde with mild derivatization conditions. *Clin Chem* **49:** 690–692.

Dhaunsi G, Paintlia MK, Kauer J, Turner R (2004) NADPH oxidase in human lung fibroblasts. *J Biomed Sci* **11:** 617–622.

Diakonov I, Schott J, Martin F, Harrichourry J-C, Escalier J (1999) Iron (III) solubility and speciation in aqueous solutions. Experimental study and modeling: Part I. Hematite solubility from 60 to 300°C in NaOH-NaCl solutions and thermodynamic properties of $Fe(OH)_4$. *Geochim Cosmochim Acta* **63:** 2247–2261.

Donaldson K, Tran L, Jimenez LA, Duffin R, Newby DE, Mills N, MacNee W, Stone V (2005). Combustion-derived nanoparticles**:** A review of their toxicology following inhalation exposure. *Part Fibre Toxicol* **2:** 10.

Flórián K, Matherny M, Nickel H, Pliešovská N, Uhrinová K (2003), Environmental characteristics of the atmosphere of residential agglomerations. II. Main, minor and trace elements in the gravitation dust sediments. *Chem Pap* **57:** 374–381.

Froschauer EM, Schweyen RJ, Wiesenberger G (2009) The yeast mitochondrial carrier proteins Mrs3p/Mrs4p mediate iron transport across the inner mitochondrial membrane. *Biochim Biophys Acta,* **1788:** 1044–1050.

Giasuddin ABM, Kanel SR, Choi H (2007) Adsorption of humic acid onto nanoscale zerovalent iron and its effect on arsenic removal. *Environ Sci Technol* **41:** 2022–2027.

Goldberg DM, Spooner RJ (1983) Glutathione reductase. In *Methods of enzymatic analysis, 3rd ed.* Bergmayer HU, ed, pp 258–265. Dearfield Beach**:** Verlag Chemie.

Green FHY, Gehr P, Lee MM, Schűrch S (2000) The role of surfactant in disease associated with particle exposure. In *Particle-Lung Interactions*. Gehr P, Heyder J, eds, pp 533–572. Marcel Dekker Inc, New York.

Guo B, Zebda R, Drake SJ, Sayes CM (2009) Synergistic effect of co-exposure of carbon black and Fe_2O_3 nanoparticles on oxidative stress in cultured lung epithelial cells. *Part Fibre Toxicol* **6:** 4.

Gurr JR, Wang AS, Chen CH, Jan KY (2005) Ultrafine titanium dioxide particles in the absence of photoactivation can induce oxidative damage to human bronchial epithelial cells. *Toxicology* **213:** 66–73.

Habig WH, Pabst MJ, Jakoby WB (1974) Glutathione-*S*-transferase. The first enzymatic step in mercapturic acid formation. *J Biol Chem* **249:** 7130–7139.

Hare JM, Stamler JS (2005) NO/redox disequilibrium in the failing heart and cardiovascular system. *J Clin Invest* **115:** 509–517.

Hauptmann N, Grimsby J, Shih JC, Cadenas E (1996) The metabolism of tyramine by monoamine oxidase A/B causes oxidative damage to mitochondrial DNA. *Arch Biochem Biophys* **335:** 295–304.

Hausmann A, Aguilar Netz DJ, Balk J, Pierik AJ, Muhlerhoff U, Lill R (2005) The eukaryotic P loop NT-Pase Nbp35: an essential component of the cytosolic and nuclear iron-sulfur protein assembly machinery. *Proc Natl Acad Sci USA* **102:** 3266–3271.

Hernández R, Zamora-Mora V, Sibaja-Ballestera M, Vega-Baudrit J, López D, Myangos C (2009) Influence of iron oxide nanoparticles on the rheological properties of hybrid chitosan ferrogels. *J Colloid Interface Sci* **339:** 53–59.

Hurd TR, Murphy MP (2009) Biological systems relevant for redox signalling and control. In *Redox signalling and regulation in biology and medicine*. Jacob C, Winyard PG, eds, pp 13–45. Wiley-VCH Verlag GmbH&Co. KGaA, Weinheim.

Jang J-H, Dempsey B, Burgos W (2007) Solubility of hematite revisited: Effects of hydration. *Environ Sci Technol* **41:** 7303–7308.

Jeng HA, Swanson J (2006) Toxicity of metal oxide nanoparticles in mammalian cells. *J Environ Sci Health* **41:** 2699–2711.

Klotz LO, Sies H (2009) Cellular generation of oxidants: relation to oxidative stress. In *Redox signaling and regulation in biology and medicine.* Jacob C, Winyard PG, eds, pp 45–61. Wiley-VCH Verlag, Weinheim, Germany.

Kruszewski M (2004) The role of labile iron pool in cardiovascular diseases. *Acta Biochim Pol* **51:** 471–480.

Li N, Hao M, Phalen RF, Hhinds WC, Nel AE (2003) Particulate air pollutants and asthma. A paradigm for the role of oxidative stress in PM-induced adverse health effects. *Clin Immunol* **109:** 250–265.

Maynard AD, Kuempel ED (2005) Airborne nanostructured particles and occupational health. *J Nanopart Res* **7:** 587–614.

Mosmann J (1983) Rapid colorimetric assay for cellular growth and survived. *J Immunol Methods* **65:** 55–63.

Muller FL, Liu Y, Van Remmen H (2004) Complex III releases superoxide to both sides of the inner mitochondrial membrane. *J Biol Chem* **279:** 49064–49073.

Műhlfeld C, Rothen-Rutishauser B, Blank F, Vanhecke D, Ochs M, Gehr P (2008) Interactions of nanoparticles with pulmonary structures and cellular responses. *Am J Physiol Lung Cell Mol Physio*l **294:** L817–L829.

Nel A, Xia T, Madler L, Li N (2006) Toxic potential of materials at the nanolevel. *Science* **311:** 622–627.

Oberdorster G, Oberdorster E, Oberdorster J (2005) Nanotoxicology**:** an emerging discipline evolving from studies of ultrafine particles. *Environ Health Perspect* **113:** 823–839.

Paoletti F, Aldinucci D, Mocali A, Caparrini A (1986). A sensitive spectrophotometric method for the determination of superoxide dismutase activity in tissue extracts. *Anal Biochem* **154:** 538–541.

Powell MC, Kanarek MS (2006) Nanomaterial health effects — Part 1: background and current knowledge. *Wisconsin Med J* **105:** 14–18.

Rothen-Rutishauser B, Schűrch S, Gehr P (2007) Interaction of particles with membranes. In *Toxicology of particles.* Donaldson K, Borm P eds, CRC, Boca Raton FL.

Sagai M, Saito H, Ichinose T, Kodama M, Mori J (1993) Biological effects of diesel exhaust particles. I. *In vitro* production of superoxide and *in vivo* toxicity in mouse. *Free Radic Biol Med* **14**, 37–47.

Sevilla M, Valdés-Solis T, Tartaj P, Fuentes AB (2009) Fabrication of mesoporous SiO(2)-C-Fe(3)O(4)/gamma Fe(2)O(3) and SiO(2)-C-Fe magnetic composites. *J Colloid Interface Sci* **40:** 230–236.

Shukla R, Bansal V, Chaudhary M, Basu A, Bhonde RR, Sastry M (2005) Biocompatibility of gold nanoparticles and their endocytotic fate inside the cellular compartment**:** a microscopic overview. *Langmuir* **21:** 10644–106654.

Stearns R, Paulauskis JD, Godleski JJ (2001) Endocytosis of ultrafine particles by A549 cells. *Am J Respir Cell Mol Biol* **24:** 108–115.

Valko M, Rhodes CJ, Moncol J, Izakovic M, Mazur M (2006) Free radicals, metals and antioxidants in oxidative stress-induced cancer. *Chem Biol Interactions* **160:** 1–40.

Yang H, Liu C, Yang D, Zhang H, Xi Z (2009) Comparative study of toxicity, oxidative stress and genotoxicity induced by four typical nanomaterials**:** the role of particle size, shape and composition. *J Appl Toxicol* **29:** 69–78.

Yano E, Yokoyama Y, Higashi H, Nishii S, Maeda K, Koizumi A (1990) Health effects of volcanic ash: a repeat study. *Arch Environ Health* **45:** 367–373.

Wang L, Nagesha DK, Selvarasah S, Dokmeci MR, Carrier RL (2008) Toxicity of CdSe nanoparticles in Caco-2 cell culture. *J Nanobiotech* **6:** 11.